Springback Analysis of Aluminum Alloy Sheet
with Special Reference to Effect of Planar Anisotropy

Takeshi UEMORI[1], Satoshi SUMIKAWA[2], Shohei TAMURA[2]

Hiroyuki AKAGI[1] and Fusahito YOSHIDA[2]

[1] Faculty of Engineering, Kindai University, 1, Takaya Umenobe, Higashi-Hiroshima, 739-2116, JAPAN

[2] Department of Mechanical System Engineering, Faculty of Engineering,
Hiroshima University, 1-4-1, Kagamiyama, Higashi-Hiroshima, 739-8527, JAPAN

Hat-shaped draw bending experiments were performed on type AA6016-T4 aluminum sheet with strong planar anisotropy. From the comparison of the experimental results of springback with the corresponding numerical simulations, the effect of planer anisotropy on springback is discussed. For the simulation, Yoshida-Uemori kinematic hardening model (F. Yoshida & T. Uemori, Int. J. Plasticity 18, 2002; Int. J. Mech. Sci., 45, 2003) incorporating with several types of anisotropic yield functions were employed. From the experiments, it was found that springback of R.D. (rolling direction) bending differs from that of T.D. (transverse direction) bending. For accurate simulation of such anisotropic behavior of springback, the selection of anisotropic yield function, as well as the modeling of the Bauschinger effect, is very important.

Keywords: Springback, Constitutive model, Bauschinger effect, Yoshida-Uemori model, Hat bending

1. Introduction

Aluminum alloy sheets have been widely used for lightweight constructions of automobile. For press forming of aluminum sheets the prediction of springback by numerical simulation is very important, since their springback is extremely large due to their nature of low elastic rigidity. Moreover, some aluminum sheets have significant planar anisotropies in r-values and the flow stresses [1-3], and they would also influence the springback.

Two of the present authors (Uemori and Yoshida [4]) pointed out that the Bauschinger effect should be taken into account for accurate numerical simulation of springback, and for its description, they proposed an advance kinematic hardening model (Yoshida-Uemori model [5-7], hereafter we call it 'Y-U model'). This model takes into account the planar anisotropy, by choosing an appropriate anisotropic yield function, as well as the Bauschinger effect and cyclic hardening characteristics. Although it is already well-known that the Bauschinger effect strongly influences the accuracy of springback analysis, there are not so many works on the effect of anisotropies on springback. This is because most of the discussions on springback have been on high strength steel sheets which have rather weak anisotropy (their r-values are usually 0.8-1.0).

In the present work, hat-shaped draw bending experiments were performed on type AA6014-T4 aluminum sheet with strong planar anisotropy. From the comparison of the experimental results of springback with the corresponding numerical simulations, the effect of planer anisotropy on springback is discussed. Several material tests of uniaxial tension, cyclic tension-compression and biaxial stretching were performed to observe anisotropic elasto-plasticity characteristics of the sheet. For the simulation, Y-U model incorporating with several types of anisotropic yield functions (Hill48 [8], Gotoh [9] and Barlat Yld2000-2d [10]) were employed.

2. Material tests to observe elasto-plasticity characteristics

Test materials used in this study was type AA6014-T4 sheet of 1.0-mm thick. Uniaxial tension tests were carried out using a servo-controlled testing machine (SHIMADZU AG-IS, load capacity is

50kN). JIS 13A-type specimen (pararell portion is 20-mm wide and 120-mm long) was used in the uniaxial tension test. Stress-strain curves and *r*-values were determined by uniaxial tension experiments in three directions (0, 45 and 90 degrees from the rolling direction).

In-plane cyclic tension-compression tests were carried out using the specimen shown in Fig.1 (a). The specimen was prepared in such a way that six sheets were adhesively bonded together (thus thickness of the specimen was 6 mm) in order to prevent buckling under compression loading. By using FE simulation, it was confirmed that parallel part uniformly deforms during the cyclic deformation. Incremental step-up cyclic straining (strain history: $0 \rightarrow +2.5\% \rightarrow -2.5\% \rightarrow +5\% \rightarrow -5\%, \cdots$) was imposed. Tests were carried out until the rupture or buckling occurs.

Biaxial stretching tests were carried out using the cruciform specimen shown in Fig.1 (b). Slits are fabricated in the arm of the specimen in order to release the deformation constraint on the central section. The uniform deformation at the center of the cruciform specimen in equi-biaxial stretching was confirmed by FE simulation (von Mises yield criterion and the Swift hardening law). Stresses, $\sigma_x = \left(P_x / A_x \right) \exp\left(\varepsilon_x \right)$ and $\sigma_y = \sigma_y = \left(P_y / A_y \right) \exp\left(\varepsilon_y \right)$, were determined by dividing the measured loads P_x and P_y by the cross sectional areas A_x and A_y ($A_x = A_y = 52 \times 1.0\text{mm}^2$), respectively. The strains, ε_x and ε_y, were measured by strain gauges (Tokyo Sokki Kenkyujo Co., Ltd., YEFCA-2) bonded on the surface at the center of the specimen. Initial yield locus and subsequent equi-plastic work loci were obtained. From the comparisons between the experimental results and the corresponding finite element calculations under several types of bi-axial tensile conditions, it is found that the estimated errors in stress are less than $\pm 3\%$ in the present bi-axial test piece.
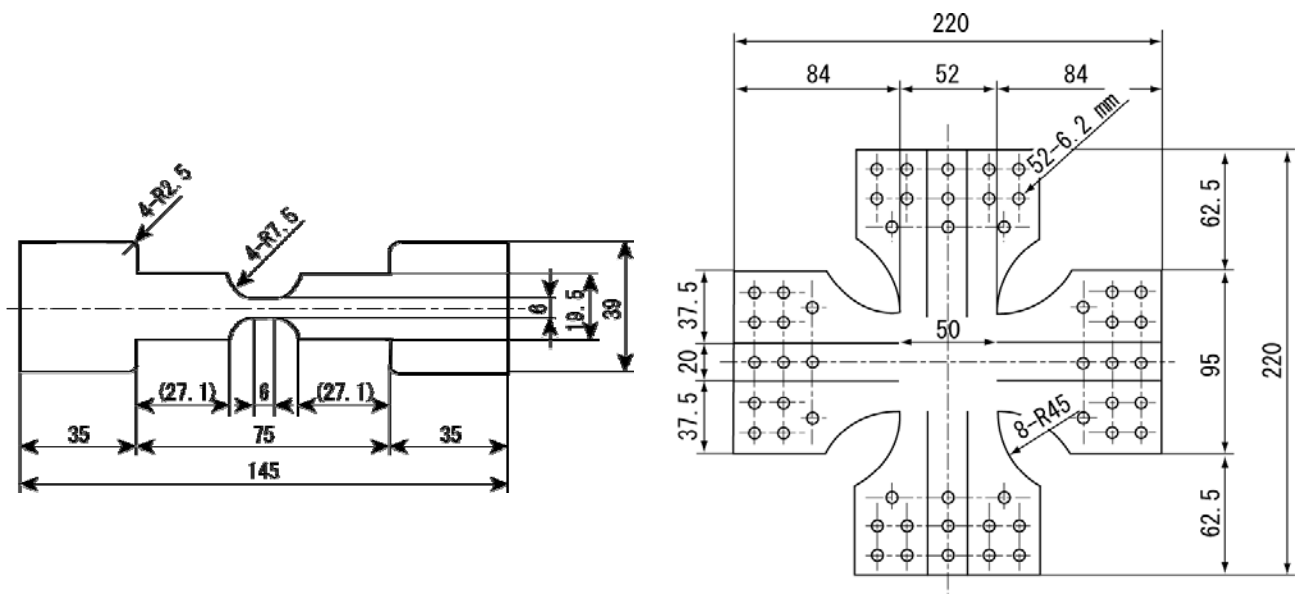
3. Constitutive modeling

3.1 Yield functions

In order to describe the orthotropic anisotropy of the sheet, the following four types of yield functions were employed:
- von Mises's isotropic yield function

$$f = \frac{1}{2}\left[\left(\sigma_{xx} - \sigma_{yy} \right)^2 + \left(\sigma_{yy} - \sigma_{zz} \right)^2 + \left(\sigma_{zz} - \sigma_{xx} \right)^2 + 3\tau_{xy}^2 + 3\tau_{yz}^2 + 3\tau_{zx}^2 \right] - Y^2 = 0 \ . \qquad (1)$$

(a) Cyclic tension-compression test　　　　(b) Biaxial stretching test

Fig.1 Schematic illustrations of in-plane specimens (in mm)

- Hill48 yield function [8]

$$f = \frac{3}{2(F+G+H)}\left[\begin{array}{c} F\left(\sigma_{yy}-\sigma_{zz}\right)^2 + G\left(\sigma_{zz}-\sigma_{xx}\right)^2 + H\left(\sigma_{xx}-\sigma_{yy}\right)^2 \\ + 2N\tau_{xy}^2 + 2L\tau_{yz}^2 + 2M\tau_{zx}^2 \end{array}\right] - Y^2 = 0 \ , \qquad (2)$$

where F, G, H, L, M, and N stand for Hill's anisotropic parameters.

- Gotoh's bi-quadratic yield function [9]

$$f = \left[\begin{array}{c} A_1\sigma_{xx}^4 + A_2\sigma_{xx}^3\sigma_{yy} + A_3\sigma_{xx}^2\sigma_{yy}^2 + A_4\sigma_{xx}\sigma_{yy}^3 + A_5\sigma_{yy}^4 \\ + \left(A_6\sigma_{xx}^2 + A_7\sigma_{xx}\sigma_{yy} + A_8\sigma_{yy}^2\right)\tau_{xy}^2 + A_9\tau_{xy}^4 \end{array}\right] - A_1 Y^4 = 0 \ , \qquad (3)$$

where $A_1 \sim A_9$ are Gotoh's anisotropic parameters. σ_{ij} and Y stand for the Cauchy stress, the initial yield stress, respectively.

- Barlat's Yld200-2d yield function [10]

$$f = \left|X_1' - X_2'\right|^M + \left|2X_2'' + X_1''\right|^M + \left|2X_1'' + X_2''\right|^M - 2Y^M = 0 \ , \qquad (4)$$

$$X' = L' : \sigma, \ X'' = L'' : \sigma \ , \qquad (5)$$

where X' and X'' stand for the stress tensor, respectively. L' and L'' are the Barlat's anisotropy interaction matrix, respectively.

3.2 Yoshida-Uremori kinematic hardening model

When the yield function at the initial state, f_0, has a general form:

$$f_o = \phi(\sigma) - Y = 0, \qquad (6)$$

where ϕ denotes a function of the Cauchy stress σ, and Y is the initial yield strength defined as the elastic limit. For function ϕ, we may choose one among existing anisotropic yield functions (e.g., [8-10]). The criterion for the subsequent yield is written by

$$f = \phi(\sigma,\alpha) - Y = 0, \qquad (7)$$

where α stands for the backstress. The associated flow rule is written as

$$D^p = \frac{\partial f}{\partial \sigma}\dot{\lambda} = \frac{\partial \phi}{\partial \sigma}\dot{\lambda}, \qquad (8)$$

where D^p denotes the plastic part of the rate of deformation. Thus the constitutive equation of plasticity is derived by determining the evolution equation of the backstress α, together with an appropriate choice of an anisotropic yield function.

As for the kinematic hardening law, Y-U model is constructed in the framework of two-surface modeling, wherein the yield surface moves kinematically within the bounding surface, as schematically illustrated in Fig.2 The bounding surface F is
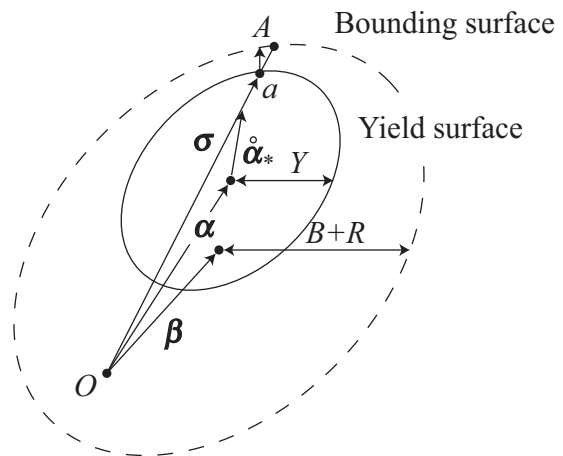

Fig.2 Two-surface model

expressed by the equation:

$$F = \phi(\boldsymbol{\sigma}, \boldsymbol{\beta}) - (B + R) = 0, \tag{9}$$

where $\boldsymbol{\beta}$ denotes the center of the bounding surface, and B and R are its initial size and isotropic hardening (IH) component. The relative kinematic motion of the yield surface with respect to the bounding surface is expressed by

$$\boldsymbol{\alpha}_* = \boldsymbol{\alpha} - \boldsymbol{\beta}. \tag{10}$$

For the evolution of $\boldsymbol{\alpha}^*$, the following equation is assumed:

$$\overset{\circ}{\boldsymbol{\alpha}_*} = C\left[\left(\frac{a}{Y}\right)(\boldsymbol{\sigma} - \boldsymbol{\alpha}) - \sqrt{\frac{a}{\bar{\alpha}_*}}\,\boldsymbol{\alpha}_*\right]\dot{p}, \tag{11}$$

$$\dot{p} = \sqrt{\frac{2}{3}\boldsymbol{D}^p : \boldsymbol{D}^p}, \quad \bar{\alpha}_* = \phi(\boldsymbol{\alpha}_*), \quad a = B + R - Y \tag{12}$$

where $\dot{p}$ is the effective plastic strain rate, defined as the second invariant of $\boldsymbol{D}^p$, and C and a are material parameters that control the rate of the kinematic hardening. For the isotropic hardening of the bounding surface, the following evolution equation is assumed:

$$\dot{R} = m(R_{sat} - R)\dot{p}, \tag{13}$$

where R_{sat} is the saturated value of the isotropic hardening stress R at infinitely large strain, and m is a material parameter that controls the rate of isotropic hardening. For the kinematic hardening of the bounding surface, the following evolution equation is assumed:

$$\overset{\circ}{\boldsymbol{\beta}} = m\left[\left(\frac{b}{Y}\right)(\boldsymbol{\sigma} - \boldsymbol{\alpha}) - \boldsymbol{\beta}\right]\dot{p}, \tag{14}$$

where b denotes a material parameter. Here, parameter m is assumed to be the same as in the evolution equation of the isotropic hardening stress. To describe the phenomenon of *workhardening stagnation* appearing in a reverse deformation, the model of non-IH hardening surface is introduced (refer to papers [6, 7]).

Besides the kinematic hardening model, the following model of plastic-strain dependent Young's modulus (Yoshida et al. [5]) was used in the calculation:

$$E = E_0 - (E_0 - E_a)\left\{1 - \exp(-\xi\varepsilon^p)\right\} \tag{15}$$

where E_0 and E_a stand for Young's modulus for virgin and infinitely large pre-strained materials, respectively, and ξ is a material constant.

4. Material behavior and its modeling

The sheet has significant planar anisotropy ($r_0 = 0.76$, $r_{45} = 0.26$, $r_{90} = 0.61$), which cannot be described by von Mises (isotropic) yield function. Fig.4 shows the initial yield loci calculated by the above mentioned several types of yield functions, together with the corresponding experimental data. Quadratic yield functions of von Mises and Hill48 fail in describing the anisotropic yield locus of the sheet, while the calculated results by higher-order yield functions proposed by Gotoh and Barlat agree well with the experimental data. Especially, Gotoh's yield function shows the best fit with the experimental data in any stress conditions. Fig.5 depicts the calculated cyclic stress strain responses by Y-U model incorporating with Gotoh's yield function. This model can describe the
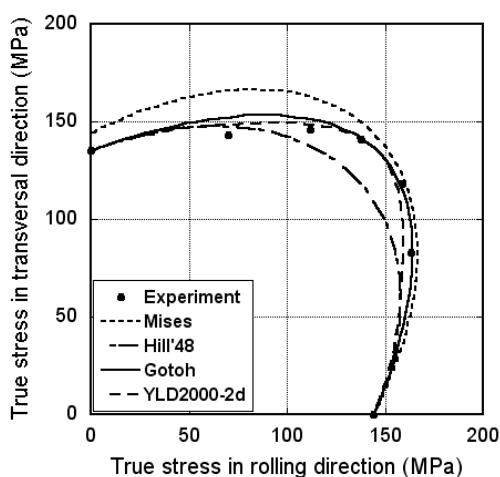
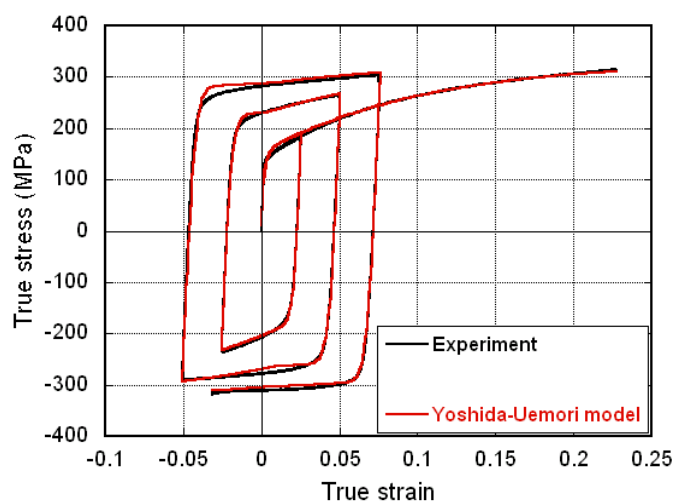Fig.3 Yield loci calculated by the four types of yield functions

Fig.4 Cyclic stress-strain responses calculated by Yoshida-Uemori model

complicated stress strain responses with the Bauschinger effect and the cyclic hardening characteristics.

5. FE simulation of springback in hat-shaped draw bending

In the present research, springback in hat-shaped draw bending was investigated. The experimental set-up is illustrated in Fig.5 Bending experiments were conducted for two directions, R.D. and T.D., of the sheet. Finite element simulations were carried out using the above mentioned four types of the yield functions: von Mises, Hill48, Gotoh and Barlat Yld2000-2d. All the calculations took into account the Bauschinger effect in the framework of Y-U model.

Y-U model incorporating with the high-ordered yield function (Gotoh or Yld2000-2d) was implemented into the FE code LS-DYNA, and using this, the FE simulation of hat bending was carried out. The same simulation using the IH + von Mises's yield function was also carried out. Fig.6 (a) shows the final forming shapes of AA6016-T4 sheet after springback in R.D. bending calculated by these models, together with the experimental result. Y-U model + anisotropic yield functions of Gotoh and Yld2000-2d show enough accurate predictions of springback, while IH + von Mises yield function underestimates the amount of springback. The change of Young's modulus is also taken into our simulations.
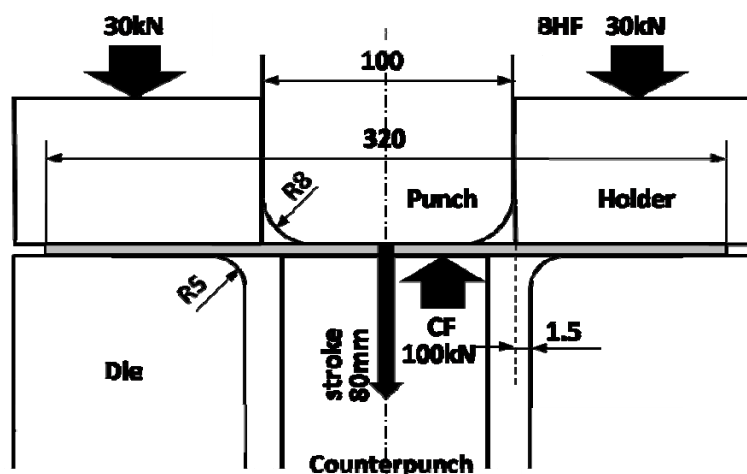

Fig.5 Experimental set-up of hat-shaped draw bending (in mm)
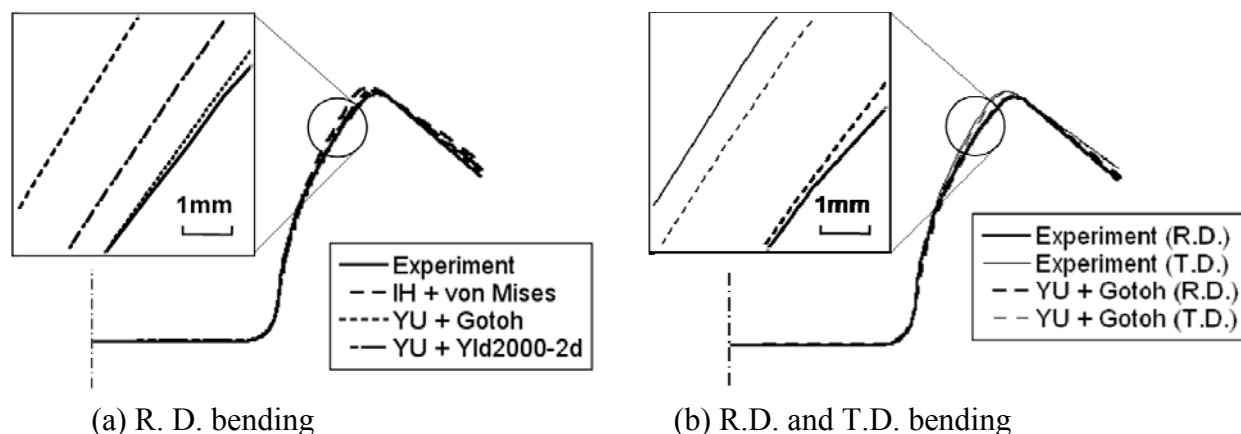
(a) R. D. bending   (b) R.D. and T.D. bending

Fig.6 Final shapes of bent sheets calculated by several types of constitutive models.

As it is seen in Fig.6 (b), the final shapes of R.D. bending and T.D. bending are apparently different. It comes from the difference in flow stress levels between R.D. bending (under plane strain condition of $\sigma_x : \sigma_y = 2:1$) and T.D. bending ($\sigma_x : \sigma_y = 1:2$). Y-U model + Gotoh yield function captures this anisotropic springback behavior.

6. Concluding remarks

Hat-shaped draw bending experiments were performed on type AA6016-T4 aluminum sheet with strong planar anisotropy. From the experiment, it was found that springback of R.D. bending differs from T.D. bending. For accurate simulation of such anisotropic behavior of springback, the selection of anisotropic yield function is very important, as well as modeling of the Bauschinger effect. For the AA6016-T4 sheet, Yoshida-Uemori kinematic hardening model + anisotropic yield functions of Gotoh and Barlat Yld2000-2d show enough accurate predictions of springback.

References

[1] F. Barlat, Y. Maeda, K. Chung, M. Yanagawa, J. C. Brem, Y. Hayashida, D. J. Lege, K. Matsui, S. J. Murtha, S. Hattori, R. C. Becker, S. Makosey: J. Mech. Phys. Solids. 45 (1997) 1727-1763.
[2] D. E. Green, K. W. Neale, S. R. MacEwen, A. Makieda, R. Perrin: Int. J. Plast. 20 (2004) 1677-1706.
[3] D. Banabic, H. Aretz, D. S. Comsa, L. Paraianu: Int. J. Plast. 20 (2004) 1677-1706.
[4] T. Uemori, T. Okada and F. Yoshida: Metals and Materials. 4 (1998) 311–314.
[5] F. Yoshida, T. Uemori, K. Fujiwara: Int. J. Plast. 18 (2002) 633-659.
[6] F. Yoshida, T. Uemori: Int. J. Plast. 18 (2002) 661-686.
[7] F. Yoshida, T. Uemori: Int. J. Mech. Sci. 45 (2003) 1687-1702.
[8] R. Hill: Proc. Roy. Soc., A193 (1948) 281-297.
[9] Gotoh, M.: Int. J. Mech. Sci. 19 (1977) 505-512.
[10] F. Barlat, J.C. Brem, J.W. Yoon, K. Chung, R.E. Dick, D.J. Lege, F. Pourboghrat, S.-H. Choi, E. Chu: Int. J. Plast. 19 (2003) 1297-1319.